

## Layer-to-Layer Height Control of Laser Metal Deposition Processes

Lie Tang, Jianzhong Ruan, Todd E. Sparks, Robert G. Landers, and Frank Liou  
Missouri University of Science and Technology  
Department of Mechanical and Aerospace Engineering  
400 West 13<sup>th</sup> Street, Rolla, Missouri 65409-0050  
{lie;tz;ruan;tsparks;landersr;liou}@mst.edu

**Abstract**—A Laser Metal Deposition (LMD) height controller design methodology is presented in this paper. The height controller utilizes the Particle Swarm Optimization (PSO) algorithm to estimate model parameters between layers using measured temperature and track height profiles. The process model parameters for the next layer are then predicted using Exponentially Weighted Moving Average (EWMA). Using the predicted model, the powder flow rate reference profile, which will produce the desired layer height reference, is then generated using Iterative Learning Control (ILC). The model parameter estimation capability is tested using a four-layer deposition. The results demonstrate the simulation based upon estimated process parameters matches the experimental results quite well. The experimental deposition using this methodology demonstrates good tracking of the height reference in terms of the finished track.

### I. INTRODUCTION

Laser Metal Deposition (LMD) is an important Solid Freeform Fabrication (SFF) technology which allows functionally graded metal parts to be deposited from three dimensional computer models [1]. Unlike traditional machining operations which build parts by material subtraction, LMD is an additive process during which the part is deposited layer by layer [2].

To deposit a part with desired geometric quality, a closed-loop process control system should be used. Laser metal deposition is a complex process, which is governed by a large number of parameters. Among these parameters, powder flow rate, laser power, and travel speed are typically used to control the process properties, such as melt pool geometry, temperature, etc. Powder flow rate sensing and closed-loop control is implemented in [3] and [4]. Both controllers are capable of producing a steady powder flow rate. Heat input control in LMD is realized by adjusting laser power using an infrared image sensing camera as feedback [5]. The controller helps to overcome the effects of thermal variations and reduces cladding geometric variations. A PID controller is developed to control the clad height in [6]. The controller is designed based on a simplified process model. The laser power and powder flow rate are kept constant during the deposition, while the clad height is controlled by adjusting the travel speed. In addition to

those controllers mentioned above, which are based on deterministic process models, there is a process controller based on statistical models. Response surface models are developed to minimize the heat affected zone (HAZ) in [7].

Process control usually requires a process model. Different models are proposed to describe the LMD process. A lumped-parameter, analytical model of material and thermal transfer is established in [8]. The model consists of three first order equations describing mass, momentum and energy balances. An elliptic shape melt pool is assumed. The model is validated by Gas Metal Arc Welding (GMAW) experiments through measurements by an infrared camera and a laser profilometry scanner. Another analytical model is developed and experimentally verified in [9]. The model concentrates on the mathematical analysis of the melt pool and establishes mass and energy balances based on one-dimensional heat conduction to the substrate. There are also some more complex models in the literature, such as the three dimensional model used to predict the thermal behavior and geometry of the melt pool in [10]. The Finite Element Method (FEM) is typically used to solve the equations in the complex models. The complex models usually require intense computational power, making them difficult to utilize in real time. The model complexity also hinders its usage for controller design.

The LMD process is characterized by an energy balance, which is affected by the part and substrate geometries, ambient temperature, etc. Therefore, the LMD process is sensitive to environmental conditions. The model parameters change as the part is being built, making a constant parameter model implausible. Also, constant height is difficult to achieve. To accommodate these limitations, a layer-to-layer height control methodology is proposed. The idea of layer-to-layer height control is to measure the part height profile between layers using a laser displacement sensor. The measured height profile and melt pool temperature are applied to identify the model parameters using PSO. The powder flow rate reference is then generated using ILC with respect to the reference height profile of the next layer. With the aid of layer-to-layer control, it is possible to make the deposition process automatic, which will help to increase productivity and reduce cost.

## II. SYSTEM HARDWARE

The LMD system consists of the following components: 5-axis CNC machine, powder delivery system, 1 kW diode laser, National Instruments (NI) real-time control system, laser displacement sensor and temperature sensor. The system setup is shown in Figure 1. The laser displacement sensor (OMRON, model Z4M-W100) has a measurement range of  $\pm 40$  mm and a minimum resolution of 8  $\mu\text{m}$ . The temperature sensor (Mikron Infrared, model MI-GA 5-LO) has a measurement range of 400 to 2500  $^{\circ}\text{C}$ . The temperature sensor is mounted on the nozzle and is used to measure the melt pool temperature during deposition. The control system is coded in NI LabVIEW and implemented on an NI real-time PXI system. A PXI 6602 counter/timer board is used for powder feeder motor angular position measurement. A PXI 6040E multifunction board with a range of  $\pm 10$  V and 12 bits of resolution is used for temperature measurement and height measurement via a laser displacement sensor. A PXI 6711 analog output board with a range of  $\pm 10$  V and 12 bits of resolution is used to input control signals to the laser and powder feeder motor amplifiers.

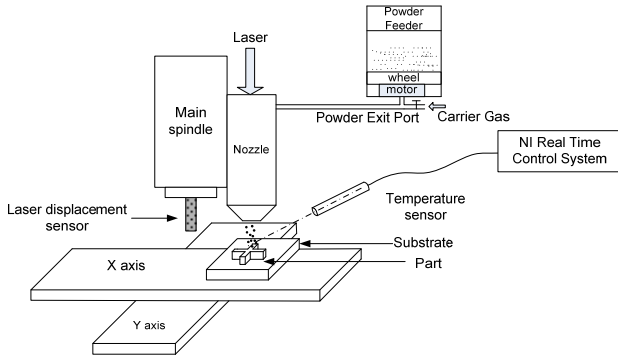


Figure 1: Laser metal deposition process system.

## III. LMD PROCESS MODEL

### A. Model description

For on-line process control, a simplified model is more desirable due to its computation efficiency. The model used in this paper is composed of three equations derived from mass, momentum and energy balances [8].

The mass balance equation is given by

$$\rho \dot{V}(t) = -\rho A(t)v(t) + \mu_m m(t) \quad (1)$$

where  $\rho$  is material density ( $\text{kg}/\text{m}^3$ ),  $V$  is bead volume ( $\text{m}^3$ ),  $A$  is cross sectional area in the direction of deposition ( $\text{m}^2$ ),  $v$  is table velocity in the direction of deposition ( $\text{m}/\text{s}$ ),  $\mu_m$  is powder catchment efficiency, and  $m$  is powder flow rate ( $\text{kg}/\text{s}$ ). The bead is assumed to be elliptical; thus, the volume and cross sectional area in the direction of deposition, respectively, are

$$V(t) = \frac{\pi}{6} w(t)h(t)l(t) \quad (2)$$

$$A(t) = \frac{\pi}{4} w(t)h(t) \quad (3)$$

where  $w$ ,  $h$ , and  $l$  are, respectively, the bead width, height, and length (m). The momentum balance is

$$\rho \dot{V}(t)v(t) + \rho V(t)\dot{v}(t) = -\rho \frac{\pi}{4} w(t)h(t)v(t)[-v(t)] + \alpha w(t) \quad (4)$$

where the parameter  $\alpha$  is given by

$$\alpha = [1 - \cos(\theta)] [\gamma_{GL} - \gamma_{SL}] \quad (5)$$

where  $\theta$  is the wetting angle (rad),  $\gamma_{GL}$  is the gas to liquid surface tension coefficient (N/m), and  $\gamma_{SL}$  is the solid to liquid surface tension coefficient (N/m). The energy balance is

$$\begin{aligned} \rho c_l \dot{T}(t)V(t) + \rho \dot{V}(t) \left[ c_s (T_m - T_0) + h_{SL} \right] = \\ -\rho \frac{\pi}{4} w(t)h(t)v(t)c_s (T_m - T_0) + \beta \mu_Q Q(t) \\ - \frac{\pi}{4} w(t)l(t)\alpha_s (T(t) - T_m) \\ - \left[ \frac{\pi}{\sqrt[3]{2}} [w(t)h(t)l(t)]^{\frac{2}{3}} \right] \left[ \alpha_G (T(t) - T_0) \right. \\ \left. + \varepsilon \sigma (T^4(t) - T_0^4) \right] \end{aligned} \quad (6)$$

where  $T$  is the average melt pool temperature (K),  $c_s$  is the solid material specific heat ( $\text{J}/(\text{kg}\cdot\text{K})$ ),  $T_m$  is the melting temperature (K),  $T_0$  is the ambient temperature (K),  $h_{SL}$  is the specific latent heat of fusion-solidification ( $\text{J}/\text{kg}$ ),  $c_l$  is the molten material specific heat ( $\text{J}/(\text{kg}\cdot\text{K})$ ),  $\beta$  is the laser-surface coupling efficiency,  $\mu_Q$  is the laser transmission efficiency,  $Q$  is the laser power (W),  $\alpha_s$  is the convection coefficient ( $\text{W}/(\text{m}^2\cdot\text{K})$ ),  $\alpha_G$  is the heat transfer coefficient ( $\text{W}/(\text{m}^2\cdot\text{K})$ ),  $\varepsilon$  is the surface emissivity, and  $\sigma$  is the Stefan-Boltzmann constant ( $\text{W}/(\text{m}^2\cdot\text{K}^4)$ ). The bead width-length relationship for the steady-state conductive temperature distribution subject to a heat source moving with constant velocity is given by

$$l(t) = X(t) + 0.25 \frac{w^2(t)}{X(t)}, \quad (7)$$

$$X(t) = \max \left[ \frac{w(t)}{2}, \frac{\beta \mu_Q Q(t)}{2\pi k (T(t) - T_0)} \right]$$

where  $k$  is the thermal conductivity constant ( $\text{W}/(\text{m}\cdot\text{K})$ ).

The experiments conducted in this paper use H13 tool steel as the deposition material. The model parameters for H13 tool steel are listed in Table 1 [9].

Table 1: H13 properties and deposition conditions.

Parameter	Symbol	Value
density ( $\text{kg}/\text{m}^3$ )	$\rho$	7760
wetting angle (rad)	$\theta$	$\pi/2$
gas to liquid surface tension coefficient (N/m)	$\gamma_{GL}$	1.94237
solid to liquid surface tension coefficient (N/m)	$\gamma_{SL}$	1.94246

solid material specific heat (J/(kg·K))	$c_s$	460
melting temperature (K)	$T_m$	1730
ambient temperature (K)	$T_0$	292
specific latent heat of fusion–solidification (J/kg)	$h_{SL}$	$2.5 \cdot 10^5$
molten material specific heat (J/(kg·K))	$c_l$	480
heat transfer coefficient (W/m <sup>2</sup> ·K)	$\alpha_G$	24
surface emissivity	$\varepsilon$	0.53
Stefan–Boltzmann constant (W/m <sup>2</sup> ·K <sup>4</sup> )	$\sigma$	$5.67 \cdot 10^{-8}$
thermal conductivity constant (W/m·K)	$k$	29
laser transmission efficiency	$\mu_O$	0.8
laser–surface coupling efficiency	$\beta$	0.15

## B. Model Simplification

Letting  $f = \frac{\beta \mu_O Q(t)}{2\pi k (T(t) - T_0)}$ , mathematical analysis

shows that  $f$  is maximum when  $Q$  is maximum (1 kW) and  $T$  is minimum (1730 K). In this case,  $f_{\max} = 4.58 \cdot 10^{-4}$  m. Experiments show that the track width is close to the laser spot diameter, which is approximately  $2.54 \cdot 10^{-3}$  m at a nozzle standoff distance of  $1.27 \cdot 10^{-2}$  m. Therefore, equation (7) becomes

$$l(t) = w(t) \quad (8)$$

## IV. CONTROLLER DESIGN

A height controller is designed based on the model described above. The height controller consists of three major parts: measurement (height and temperature), system identification, and powder flow rate reference generation. The height and temperature profiles are measured using the laser displacement and temperature sensors, respectively. The measurement data, together with the measured powder flow rate during the previous layer, are used as inputs to the system identification program, which is based on PSO [11], to estimate model parameters. Since the estimated model parameters are only applicable to the deposition of the last layer, they are further predicted using EWMA so the model can be used to predict the deposition of the next layer. The powder flow rate reference profile, which will produce the designated layer height reference, is then generated using ILC.

### A. System identification based on PSO

Particle swarm optimization is an evolutionary computational technique based on swarm intelligence. In the particle swarm algorithm, the trajectory of each particle (i.e., candidate solution to the optimization problem) in the search space is adjusted according to its own experience and the experience of the other particles

in the swarm. In this paper, it is applied to estimate the model parameters based on measured height and temperature profiles. The LMD process is governed by a number of process parameters, among which heat transfer coefficient, surface emissivity, thermal conductivity constant, convection coefficient, powder catchment efficiency, etc. are sensitive to the environment. Limited by the process feedback (height and temperature), only two process parameters, convection coefficient and powder catchment efficiency, are estimated. These two parameters play important roles in determining the melt pool temperature and height. Also in comparison with the other parameter combinations, this combination produces an excellent match with the experimental data.

The PSO algorithm is applied to determine the optimal values of  $\alpha_s$  and  $\mu_m$  based on the height and temperature feedback. Assume the swarm consists of  $n$  particles and the position and velocity vectors of particle  $i$  are given by  $X_i = [\alpha_{si}, \mu_{mi}]$ ,  $i = 1, 2, \dots, n$  and  $V_i = [v_{\alpha_i}, v_{\mu_i}]$ ,  $i = 1, 2, \dots, n$ , respectively. The position vector represents the current solution found by each particle, while the velocity vector shows how the solution will change in the next iteration.

The identification algorithm steps are as follows:

- (1) Randomly initialize the position and velocity vectors of particle  $i$  as  $X_i(0) = [\alpha_{si}(0), \mu_{mi}(0)]$  and  $V_i(0) = [v_{\alpha_i}(0), v_{\mu_i}(0)]$ ,  $i = 1, 2, \dots, n$ , respectively, and compute the fitness  $J$  of each particle by comparison of the height and temperature feedback with the deposition process simulation results using a 4<sup>th</sup> order Runge–Kutta method. In this paper, the fitness  $J$  is

$$J = \sum_{j=1}^N w_h (h_m(j) - h_s(j))^2 + \sum_{j=1}^N w_T (T_m(j) - T_s(j))^2 \quad (9)$$

where  $N$  is the total sample number,  $w_h$  is the height error weight,  $h_m$  is the measured height,  $h_s$  is the simulated height,  $w_T$  is the temperature error weight,  $T_m$  is the measured temperature, and  $T_s$  is the simulated temperature. Take the current position of each particle as its initial personal best position  $P_i(0)$  with best fitness  $JP_{best_i}(0)$ ,  $i = 1, 2, \dots, n$ , and compare the fitness of all particles in the group to find the initial global best position  $P_g(0)$  and corresponding initial global best fitness  $JG_{best}(0)$ .

- (2) Update the current iteration number  $b$  and inertial weight with  $w(b)$

$$b = b + 1, \quad w(b) = w_i - \left( \frac{w_i - w_f}{b_{\max}} \right) \cdot b \quad (10)$$

where  $b_{\max}$  is the maximum iteration number. The initial and final values of the inertia weight, respectively, are 0.9 and 0.4.

- (3) Update the position and velocity, respectively, of each particle

$$V_i(b+1) = w(b)V_i(b) + c_1 r_1 (P_i(b) - X_i(b)) + c_2 r_2 (P_g(b) - X_i(b)), \quad i=1,2,\dots,n \quad (11)$$

$$X_i(b+1) = X_i(b) + V_i(b+1), \quad i=1,2,\dots,n \quad (12)$$

The acceleration coefficients  $c_1$  and  $c_2$ , respectively, are 0.2 and 0.2. The parameters  $r_1$  and  $r_2$  are random numbers in the range  $[0,1]$ .

- (4) Evaluate the fitness of each particle  $J_i(b)$ , and compare it with its previous personal best fitness value  $JPbest(b-1)$ . If  $J_i(b) < JPbest(b-1)$ , then  $P_i(b) = X_i(b)$  and  $JPbest_i(b) = J_i(b)$ . Compare  $J_i(b)$  with the previous global best fitness  $JGbest(b-1)$ . If  $J_i(b) < JGbest(b-1)$ , then  $P_g(b) = X_i(b)$  and  $JGbest(b) = J_i(b)$ .
- (5) Compare  $JGbest(b)$  with  $JGbest(b-1)$ . If  $JGbest(b) = JGbest(b-1)$ , then let  $c = c+1$ . If  $JGbest(b) \neq JGbest(b-1)$ , then  $c = 0$ . If  $c > C_{set}$ , then randomly select  $\delta(\leq n)$  particles from the group and reinitialize. Here  $C_{set}$  is a designated natural number. If there is no fitness improvement in the past  $C_{set}$  iterations, the reinitializing process will be activated.
- (6) If  $b < b_{max}$ , then go to step (2), otherwise stop.

Similar to other optimization algorithms such as genetic algorithm, simulated annealing, etc., PSO can also become trapped at a local minimum. Here step (5) is employed to avoid local minima. The idea originates from the mutation operation used in genetic algorithms. In genetic algorithms, mutation is a random modification of a randomly selected potential solution. It guarantees the possibility of exploring the space of solutions for any initial solution space and avoiding local minima. Here the reinitializing process is designed to fulfill the same purpose.

#### 4.2 Model parameters prediction using EWMA

With the PSO algorithm described above, the parameters,  $\alpha_s$  and  $\mu_m$ , are estimated for the current layer; however, they are not applicable to the next layer. To predict the parameter values at the next layer, Exponentially Weighted Moving Average (EWMA) is used. The prediction is described by

$$P_{l+1} = A \cdot E_l + (I - A) \cdot P_l, \quad l=2,\dots \quad (13)$$

$$P_2 = E_1 \quad (14)$$

where  $l$  is the layer number,  $P_{l+1} = [\alpha_{sp}(l+1), \mu_{mp}(l+1)]$  is the vector of predicted parameters at layer  $l+1$ ,  $E_l = [\alpha_{se}(l), \mu_{me}(l)]$  is the vector of estimated parameters using PSO at layer  $l$ ,  $I$  is the  $2 \times 2$  identity matrix, and  $A$  is a  $2 \times 2$  diagonal matrix consisting of smooth factors for each parameter. In this paper  $A = \begin{bmatrix} 0.5 & 0 \\ 0 & 0.5 \end{bmatrix}$ , which is selected empirically.

#### 4.3 Powder Flow Rate Generation using ILC

Iterative Learning Control (ILC) has been widely applied in robotics for tracking repeated motion contours. The idea is to adjust the controller output according to the tracking error in the previous iterations and, since the motions are usually repeated, the controller output will converge to a certain value which will produce an acceptable tracking result.

The control law is

$$u_{j+1}(i) = f(e_j, e_{j-1}, \dots, e_{j-n}, u_j, \dots, u_{j-n}) \quad (15)$$

so that the learning convergence, i.e.,  $\lim_{j \rightarrow \infty} \|e_j\| \rightarrow 0$  and

$\lim_{j \rightarrow \infty} \|u^* - u_j\| \rightarrow 0$  is achieved at an acceptable rate. The parameter  $j$  is the iteration number, and  $i$  is the sample index.

Unlike the usual applications described above, ILC is used to generate the powder flow rate reference profile in this paper. The control law applied in this paper was first proposed by Arimoto *et al.* [12] and is

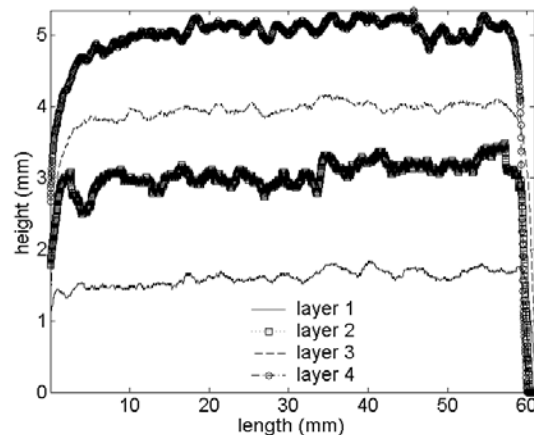
$$m_{j+1}(i) = m_j(i) + \gamma e_j(i+1) \quad (16)$$

The powder flow rate at time  $i$  and iteration  $j+1$  is calculated from the powder flow rate at time  $i$  and the previous iteration  $j$  and a corrective term which is a learning gain  $\gamma$  multiplied by the shifted tracking error  $e_j(i+1)$  from the previous iteration. One thing that should be noted is that in this procedure ILC utilizes virtual deposition (with the help of process model) to generate the powder flow rate reference.

### V. EXPERIMENTAL STUDIES

#### A. Process model parameter estimation

To test the model parameter identification methodology, a four-layer single track wall is deposited using H13. The powder flow rate is  $0.83 \cdot 10^{-4}$  kg/s, the laser power is 700 W, the table travel velocity is  $2.1 \cdot 10^{-3}$  m/s, and the nozzle standoff is  $1.27 \cdot 10^{-2}$  m. The track length is approximately 60 mm. The measured track height and melt pool temperature are shown in Figure 2.



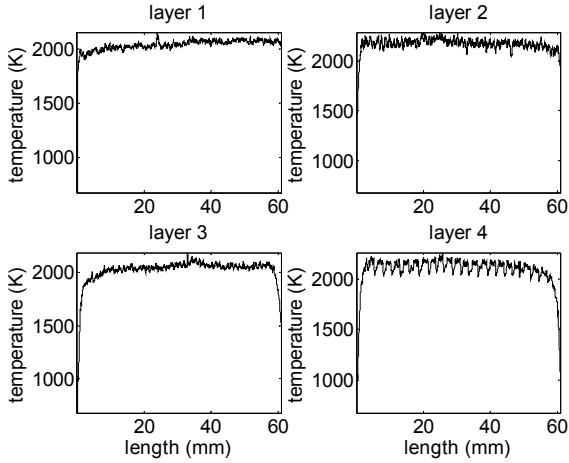


**Figure 2: Measured track height and temperature profiles for four layers.**

The model parameters ( $\alpha_s$  and  $\mu_m$ ) are estimated using the PSO algorithm for all four layers. The identification program implemented with Visual C++ 6.0 runs on a computer platform with the following settings: CPU – Celeron M (1.40 GHz), Memory – 448 MB, System – Windows XP professional edition (2002). The particle number and iteration number are both 100. The average computation time is 68.8 seconds and the standard deviation is 2.9 seconds. The estimated parameter values are given in Table 2. The experimental results are compared with the simulation results in Figure 3.

**Table 2: Estimated model parameters for all four layers.**

Layer	$\alpha_s$ (W/m <sup>2</sup> ·K)	$\mu_m$
1	$2.46 \cdot 10^4$	0.62
2	$1.87 \cdot 10^4$	0.56
3	$3.55 \cdot 10^4$	0.35
4	$2.59 \cdot 10^4$	0.43

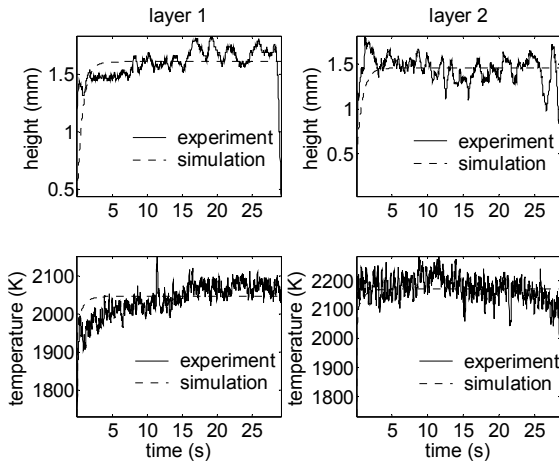


**Figure 3: Experimental and simulation results for layers 1 and 2.**

The results show that the simulation results using estimated parameters match the experimental results quite well except for slight variations, which are due to unmodeled process dynamics. It should also be noted that parameters experience significant changes between layers indicating the necessity of parameter prediction.

## 5.2 Layer-to-Layer Height Control Experimental

With the system parameter estimation capability and powder flow rate reference generation successfully verified, the layer-to-layer height control methodology is implemented and a single track with a desired height of 4 mm is deposited. The height reference profile for each layer is generated using the following equation

$$h_r(k) = h_a + 0.5 \cdot h_m(k) \quad (17)$$

where  $h_r$  is the height reference profile for the next layer,  $h_a$  and  $h_m$  are the average track height and track height profile of the current layer, respectively. The deposition results are shown in Figure 4.

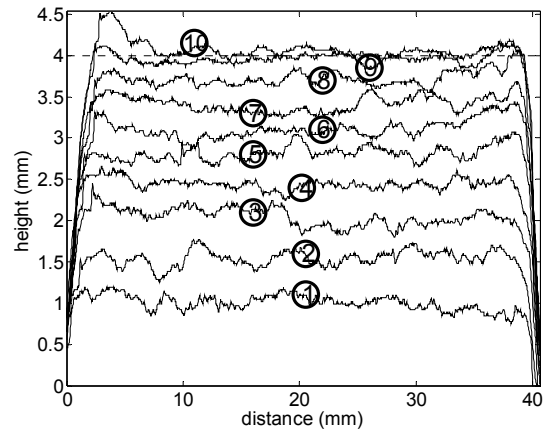


**Figure 4: Height profile of each layer in a single track deposition with height control.**

The total layer number is 10 and average height of the finished track is 4.04 mm. The average height error and the error standard deviation of each layer are listed in Table 3.

**Table 3: Height error average and standard deviation**

Layer	Average height error (mm)	Error standard deviation (mm)
1	N/A	N/A
2	0.095	0.10
3	0.10	0.12
4	0.078	0.10
5	0.097	0.11
6	0.17	0.14
7	0.15	0.12
8	0.15	0.12
9	0.067	0.078
10	0.081	0.12

To show how the methodology works between layers, the results for layer 9 are shown in Figure 5. Good tracking of the height reference is shown in the top subplot. The corresponding powder flow rate measurement and reference profiles are shown in the bottom subplot. The average height error is 0.067 mm and the standard deviation is 0.078 mm. The large height errors, which happen at the start and end of the deposition, are due to the laser displacement sensor, which averages the height in its measurement window. Due to the slow response of the powder delivery system, the powder feeder controller cannot track a fast changing reference very well. The height tracking error is due to a combination of following causes: unmodeled process dynamics, powder flow rate reference tracking errors, and model parameter prediction error.

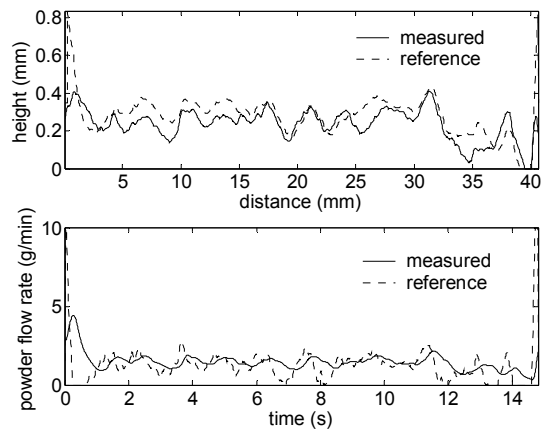


**Figure 5: comparison between height/powder flow rate reference and their measured value**

## VI. SUMMARY AND CONCLUSIONS

A LMD height controller design methodology is presented in this paper. The height controller utilizes the PSO algorithm to estimate the model parameters from measured temperature and track height profiles between layers. The model parameters are then further predicted using EWMA to account for the process parameter variations. With the predicted model, the powder flow rate reference profile, which will produce the designated layer height profile, is then generated using ILC. The model estimation capability of the methodology is verified experimentally. The experimental result of a single track deposition demonstrates a good tracking of the height reference regarding the finished track, although the height controller performance may vary between layers.

## ACKNOWLEDGMENT

The authors would like to acknowledge the financial support of the Intelligent Systems Center at Missouri University of Science and Technology.

## REFERENCES

- [1] Choi, J., 2002, "Process and Prosperities Control in Laser Aided Direct Metal/Materials Deposition Process," *Proceedings of IMECE*, New Orleans, Louisiana, November 17–22, pp. 1–9.
- [2] Griffith, M.L., Keicher, D.M., Atwood, C.L., Romero, J.A., Smegeresky, J.E., Harwell, L.D., and Greene, D.L., 1996, "Free Form Fabrication of Metallic Components Using Laser Engineered Net Shaping (LENS)," *Solid Freeform Fabrication Symposium*, Austin, Texas, pp. 125–131.
- [3] Hu, D. and Kovacevic, R., 2003, "Sensing, Modeling and Control for Laser-Based Additive Manufacturing," *International Journal of Machine Tools and Manufacture*, Vol. 43, No. 1, pp. 51–60.
- [4] Li, L. and Steen, W.M., 1993, "Sensing, Modeling and Closed Loop Control of Powder Feeder for Laser Surface Modification," *ICALEO*, pp. 965–975.
- [5] Hu, D., Mei, H., and Kovacevic, R., 2001, "Closed Loop Control of 3D Laser Cladding Based on Infrared Sensing," *Solid Freeform Fabrication Proceedings*, Austin, Texas, pp. 129–137.
- [6] Fathi, A., Durali, M., Toyserkani, E., and Khajepour, A., 2006, "Control of the Clad Height in Laser Powder Deposition Process using a PID Controller," *Proceedings of IMECE*, November 5–10, Chicago, Illinois, USA.
- [7] Keicher, D.M., Jellison, J.L., Schanwald, L.P., Romero, J.A., and Abbott, D.H., 1995, "Towards a Reliable Laser Spray Powder Deposition System through Process Characterization," *27<sup>th</sup> International SAMPE Technical Conference*, October 9–12, pp. 1009–1018.
- [8] Doumanidis, C. and Kwak, Y–M., 2001, "Geometry Modeling and Control by Infrared and Laser Sensing in Thermal Manufacturing with Material Deposition," *Journal of Manufacturing Science and Engineering*, Vol. 123, pp. 45–52.
- [9] Han, L., Liou, F.W., and Musti, S., 2005, "Thermal Behavior and Geometry Model of Melt Pool in Laser Material Process," *Journal of Heat Transfer*, Vol. 127, pp. 1005–1014.
- [10] Pinkerton, A.J. and Li, L., 2004, "Modelling the Geometry of a Moving Laser Melt Pool and Deposition Track via Energy and Mass Balances," *Journal of Physics D: Applied Physics*, Vol. 37, pp. 1885–1895.
- [11] Kennedy, J. and Eberhart, R.C., 1995, "Particle Swarm Optimization," *IEEE International Conference on Neural Networks*, Perth, Australia, November, pp. 1942–1948.
- [12] Arimoto, S., Kawamura, S., and Miyazaki, F., 1984, "Bettering Operations of Robots by Learning," *Journal of Robotic Systems*, Vol. 1, pp. 123–140.